IJST EXPLORE International Journal of Science and Technology
CENTRE OF PROFESSIONAL RESEARCH PUBLICATIONS
ISSN 2049-7318

International Journal of Science and Technology Volume 2 No. 4, April, 2013

An Assessment of Critical Loadings and Member sizing for the Design of Structural Support for a Solar Tracking Bi-Focal Collector System

[1]Abdulrahim A. T. , [2]Onundi, L. O. and [3]Diso, I. S.
[1]Department of Mechanical Engineering, University of Maiduguri, Nigeria.
[2]Department of Civil and Water Resources Engineering, University of Maiduguri, Nigeria.
[3]Department of Mechanical Engineering, Bayero University, Kano, Nigeria.

ABSTRACT

The study focuses on the assessment of critical loadings and member sizing for the design of structural support for a solar tracking bi-focal collector system. Support structure that is capable of holding the solar collectors under various operating conditions comprises of a mild steel rotating shaft for supporting the two number solar collectors, support frame that permits azimuth rotation and collective rotation of the solar collectors. Procedure recommended by the American Institute of Steel Construction (AISC) was followed in this study, while RISA 3D software was used for the analysis of the structural system at the serviceability limit state because of the dynamic nature of some of the acting forces. A finite element solution was derived through the assumption of a triangular element stiffness matrix for a co-planner (two dimensional) stress formulation as a model. A single 25 x 25 x 3mm (1.2kg/m) equal angle iron proved adequate and satisfactory for all the members except the shaft which is CHS48.3x5mm (5.34kg/m). No excessive stress, deformation or any other related dynamic sensitive considerations proved to have adverse influence on the structural stability, durability, reliability or quality assurance capabilities of the solar tracking system. Therefore, a procedure for the preliminary sizing of members and application of finite element method for the design and stability of structural support for a solar tracking bi-focal collector system have been achieved and same is recommended for larger magnitudes.

Keywords: *Solar collectors, Support Structure, Static, Dynamic, Loadings*

1. INTRODUCTION

Solar collectors for solar energy are generally categorised as either concentrating or non-concentrating solar systems. Concentrating solar collectors typically comprise of a reflector for reflecting and concentrating received solar radiation towards an absorber (Muller-Steinhagen, 2003). The absorber may include a conduit for carrying a heat transfer fluid for absorbing solar thermal energy. The reflector is either in form of a circular dish with the focal position above the centres of the dish, or a trough-like, parabolic reflector which produces a line focus along the length of the reflector. Focusing or concentrating solar collectors typically require some type of sun tracking mechanism and tracking control system to vary the orientation of the collector to maintain the focal position of the solar radiation of the absorber surface (Cooper, 1972; Duffie and Beckman, 1974 and Magal, 1993).

The bi-focal solar tracking collector system is an example of a dish-like solar collector system linked together to increase generating capacity instead of it been used independently. The provision of suitable and appropriate support structure for the bi-focal solar tracking collectors is important in order to guaranty the system functionability during operation or service life span. It is essential for the structure that supports the parabolic mirrors and absorbing tube to have the necessary torsional stiffness and flexural rigidity to maintain the precision of the focus of the energy capture surface on the absorbing tube, which is particularly important taking into account that; solar collector system is accompanied by solar tracking mechanisms, in order to achieve optimum production of energy (Abdulrahim *et al.;* 2012).

Several attempts have been made to provide structural supports for solar collectors in this part of the world but such efforts were mostly directed towards single dish solar collectors with manual tracking (Ajiya, 1995; Mshelbwala, 1996; Pelemo *et al.,* 2002 and Dahiru *et al.,* 2007). These structural supports cannot be adopted for a bi-focal solar tracking collector system because of the increased number of solar collectors. Apart from this, there is some little torsional stiffness consideration vital for the stability, durability and reliability of the structural system; since they are not associated with a moving tracker device but could in some ways influence the efficiency or optimum performance of the collectors. The present study is therefore aimed at designing appropriate structural support for the solar tracking bi-focal collector system. A support structure that will be capable of holding the solar collectors, stable enough to support the bi-focal collectors under a wide range of critical loading conditions; including violent or extreme cases of pulsating

IJST © 2013– IJST Publications UK. All rights reserved.

wind speeds that might occur at various locations of the World. Such structural supports must be capable of simultaneously withstanding the likelihood of increase in the Reynolds number (Re) with increase in wind speeds at the level of the parabolic disk as this is important to satisfy the general stability requirements of the structural system. This concerned is particularly important since low Reynolds number (e.g. 0.5), usually produces the inertia effects which are negligible but between 2 and 30, separation of boundary layer occurs with symmetrical eddies rotating in opposition to one another are formed. As the Reynolds number increases, this process is intensified and the formation of wake of discreet rows of vortices is developed. At this stage, the contribution of drag profile is three-quarters (Douglas *et al.*, 1980). It will then be seen that shedding of each vortex produces circulation and hence, gives rise to a lateral force that could cause excessive vibration on the body; if this particular influence on the structural stability and serviceability is not properly investigated and curtailed.

2. METHODOLOGY

The Solar tracking bi-focal collector system consist of these component parts which must be supported; two collectors and the receivers; the driving and counter weights; and the tracking mechanism as well as other auxiliary parts necessary for proper operation of the system. The required structural supports are the rotating support shaft, the framework and the arms linkages.

2.1 Design of the Rotating Support Shaft

The rotating support shaft was design by computing the magnitudes of various loads acting on it at the serviceability limit state since the resultant forces of the driving shaft, the chain drive system and the pulsating wind loadings are expected to be time dependent or dynamic in nature; hence an elastic design of the structural system is assumed. The corresponding distances between the supports and the positions of action of the loads were respectively determined. For this study, a hollow shaft was chosen. The appropriate diameter of the shaft was obtained from the expression given by (Khurmi and Gupta, 2004; Allen e*t al.*, 1982).

$$M = \frac{\pi}{32} \times \sigma_b (d_0)^3 (1 - k^4) \quad (1)$$

Where,

M = Maximum elastic bending moment
σ_b = Allowable bending stress
d_o = Outside diameter
k = Ratio of inside and outside diameters of the shaft

2.2 Design of Framework Support Structures

The framework support structures consist of the stem (super structure) and base (sub structure) which is uniting the two separate collectors. The procedure specified for the design of the framework support structures by the American Institute of Steel Construction (AISC) as presented by Shigley and Mischke (2001) has been adopted for the design of the structural support of the solar collectors system.

The AISC defines allowable stresses as the specified minimum strengths reduced by multiplication factors varying from 40 to 90 percent to ensure safety. Designating allowable normal stress as σ_{all} and allowable shear stress as τ_{all}, the relationship between allowable stresses and specified minimum strengths using the AISC code are specified as follows:

TENSION $0.45\ Sy \leq \sigma_{all} \leq 0.60 Sy$ (2a)

SHEAR $\tau_{all} \leq 0.40\ Sy$ (2b)

BENDING $0.60\ Sy \leq \sigma_{all} \leq 0.75\ Sy$ (2c)

BEARING $\sigma_{all} = 0.90\ Sy$ (2d)

Sy = the characteristic yield strength of mild steel

The loads or forces used to determine the afore-mentioned stresses are as follows:

$$F = \Sigma W_d + \Sigma W_L + \Sigma k F_L + F_w + \Sigma F_{misc} \quad (3)$$

Where,

ΣW_d - The sum of dead loads which consist of the steel work, materials fastened to it and parts supported by it.

ΣW_L - The sum of all the stationary or static live loads which includes the weight of equipment, occupants, fixtures, (and the snow load if specified by applicable code).

F_L - The force or the resultant of forces due to equipment that may cause impact or dynamic loading here considered as live load.

K - This is a service factor defined in Table 1.

F_w - The wind load on the structure (The appropriate guidelines specified by local or regional code can be utilized).

ΣF_{misc} - This term must be included in some localities to account for the effects of earthquakes, hurricanes, or other extraordinary regional conditions that might affect the structural stability of the system.

The final step in the AISC procedure recommends the selection of geometrical dimensions of members that

IJST © 2013– IJST Publications UK. All rights reserved.

ensure, the design stresses computed from the force, F does not exceed the allowable stress given as follows:

$$\sigma_n \leq \sigma_{all} \text{ or } \tau_s \leq \tau_{all} \quad (4)$$

Where

σ_n and τ_s are the design values of the normal and shear stresses respectively.

Table 1: AISC Service Factor for Use in Equation 3

For support of elevators	k = 2.00
For cab-operated travelling-crane support girders and their connection	k = 1.25
For pendant-operated travelling-crane support girders and their connections	k = 1.10
For supports of light machinery, shaft or motor driving	k ≥ 1.20
For support of reciprocating machinery or power driven unit	k ≥ 1.50
For hangers support floors and balconies	k = 1.33

Sources: Shingley and Mischke (2001)

3. DESIGN ANALYSIS

3.1 Rotating Support Design

Various loads acting on the rotating support caused by the weights of individual components of the system are:

Weight of the vertical component of the 1st solar collector, F_A = 190.18N

Weight of the vertical component of the 2st solar collector, F_G = 190.18N

Driving weight, F_C = 625.3N

Counter weight, F_D = 204.5N

Weight of the iron bearing chain, F_F = 36.77N

i. Total load acting downward = 1246.93N

ii. Reactions at the bearings, R_1=737.87N and R_2=509.062N

iii. Bending moment at various points are shown in Fig 1b

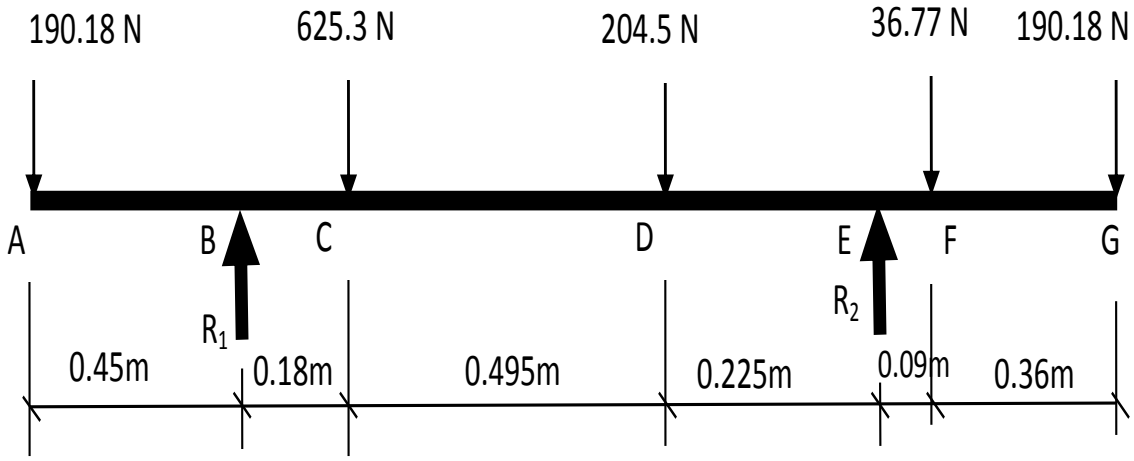

Figure 1a : Various Loads acting on the Rotating Shaft Support

IJST © 2013– IJST Publications UK. All rights reserved.

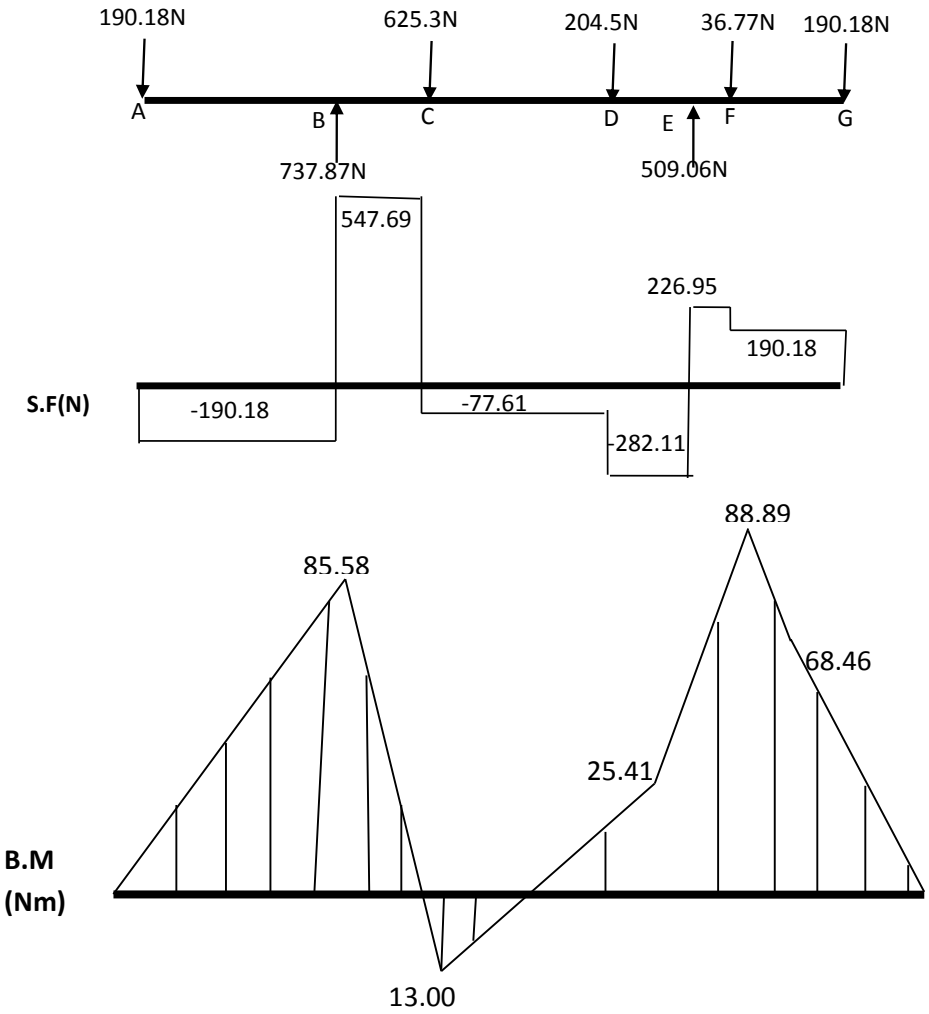

Figure 1b: The Line Diagram of Loads, Shearing Forces and Bending Moment Diagrams

The maximum bending moment of 88.89Nm occurring at point E is taken as the design maximum elastic bending moment. Using equation (1) above, computed internal and external diameter s of the shaft are 45.5mm and 46.4mm respectively. For this study, a shaft of 49mm external and 43mm internal diameters is selected.

i) For the present study, the sum of the dead loads (ΣW_d) and stationary or static live loads (ΣW_L) have been resolved and computed to produced the reactions R_B (737.5N) and R_E (509.06N) on collectors' rotating shaft support.

ii) The forces introduced by the weight of the driving shaft and the chain drive system are regarded as force or the resultant forces due to equipment or parts that may cause impact or dynamic loading, F_L. The appropriate service factors were used to multiply these forces.

iii) Driving Shaft Force, F_L = mass of shaft x acceleration due to gravity
= 19.53kg x 9.81m/s^2
= 191.49N

F_L due to driving shaft = 191.49N
k for driving shaft is taken as 1.2 from Table 1
kF_L = 1.2 x 191.49 = 229.799N
$kF_L \approx$ 230N

The kF_L (230N) is distributed between the two reactions (R_B and R_E) and are expected to be taken care off by each side of the support structure. Therefore;

- Expected support reaction at point B is:

  $R_B v$ = 737.5+115 = 852.5N and

- Expected support reaction at point E is:
  $R_E v$ = 509.06 + 115 = 624.06N

Therefore, loads acting on the support bearings were approximated as 0.86KN and 0.63KN for points B and E respectively in order to accommodate other uncomputed and unforeseen loads such as bearings and bearing housings weight, bolts and nuts weights etc. The force due

IJST © 2013– IJST Publications UK. All rights reserved.

to chain drive system is the sum of the total forces introduced by each component part of the system. The total mass of the component parts is 16.989kg. This is made up of the masses of the Shafts (0.9kg), Small Sprockets (0.049kg), Big Sprocket (0.71kg), Cog wheel (0.093kg), Chains (0.75kg), Pendulum and Anchor (1.4kg), Frame (12kg), Escapement gear (0.3kg), and the Bolts and Nuts (0.787kg).

Hence, the force due to chain drive,

$F_L = 16.989 \times 9.81$
$F_L = 166.662$ N

For the chain drive, k is taken as 1.2 from Table 1.0

$\therefore kF_L = 166.662 \times 1.2 = 199.995$N
$kF_L \approx 200$N.

This force $kF_L \approx 200$N is to be supported by member(s) on one side of the support structure.

3.2 Derivation of the Wind Load

Asante-Nimako (1988) has critically examined the recommendations made by the Nigerian Code of practice NCP1: Part 3 and the BSI Code of Practice CP3: chapter V: Part 2, (1977) in respect of wind load estimation for structures in Nigeria and concluded that the provisions made for wind load consideration in the Nigerian Code of Practice NCP1 (1973) is very inadequate. Hence, for the present study the recommendations made by the BS1 code of practice CP3: Chapter V: Part 2, (1977) and BS 6399, (2004) were adopted.

The recommendations made by the BS1 Code of Practice CP3: chapter V: Part 2 (1977) in estimating the wind loads on a structure follows the procedure below:-

1. Estimate the basic wind speed V_w, appropriate to the area or district where the structure is to be built. This is done using the isopleths map developed by Soboyejo, (1971) and Onundi, (2010) for Nigeria.
2. Determine the design wind speed Vs, by multiplying the Basic wind speed by the topography factor S_1, the terrain factor S_2 and the statistical factor S_3 :

$$Vs = V_w \times S_1 \times S_2 \times S_3 \quad (5)$$

3. Convert the Design Wind speed to dynamic pressure, q using the relationship

$$q = KVs^2 \quad (6)$$

4. The dynamic pressure q is converted into Load P using either pressure coefficients or force coefficients. Using pressure coefficients C_p, gives the pressure exerted at any particular point on the structure surface as

$$P = C_p q \quad (7)$$

And the force coefficient C_f , gives the pressure P, exerted on the structure as a whole

$$P = C_f q \quad (8)$$

For this design, the effective height of the structural support is taken as 1.5m in order to accommodate:

(i) The half dish diameter when it is facing horizontal direction, at the end of the day,

(ii) The length of the driving weight wire rope,

(iii) The length of the counter weight support and

(iv) The length of the pendulum.

The clear span of the supports is taken as 1.5m to accommodate the two solar collectors when positioned side by side.

Two vertical members were selected for the supports as reactions for the driving shaft. The span of the stem is taken as 0.4m so as to provide enough space for positioning the chain drive system without compromising general stability.
For this study, a preliminary sizing of 35 x 35mm (1.65 kg/m) equal angles mild steel was selected as the vertical, horizontal and braces or wind lattice members of the support structure subject to structural analysis for confirmation for final suitability.

3.3 Estimation of the Wind Load

a) The maximum loaded area of the support system is considered as follows :

- Area of vertical members (2 No.); 2 x 0.035 x 1.5 = 0.105m^2
- Area of Horizontal member (1 No.); 0.035 x 1.8 = 0.063m^2
- Area of driving weight = 0.02m^2
- Area of the collectors (2 No.); 1.52 x 2 = 3.06m^2

Total loaded area, A = 0.105 + 0.063 + 0.02 + 3.06
A = 3.248m^2

b) Design wind load, $Vs = V_w \times S_1 \times S_2 \times S_3$

The basic wind speed V_w for Maiduguri is taken 50 m/s (Asante-Nimako, 1988 and Onundi, 2010).

- The topography factor, S_1 is taken as 1.1 (Hughes, 1976)

IJST © 2013– IJST Publications UK. All rights reserved.

- The terrain factor, S_2 is taken as 0.83 (Hughes, 1976)

- The statistical factor, S_3 is taken as 1.05 (Hughes, 1976)

$\therefore$ Vs = 50 x 1.1 x 0.83 x 1.05 = 47.94 m/s

c) Dynamic pressure, $q = kVs^2$

where

k= 0.613 for SI units (Hughes, 1976)
$q = 0.613 \times (47.94)^2$
$q = 1408.4\ N/m^2$

d) Total wind Load, F

$F = C_f\ q\ A$

The force coefficient C_f is taken as 1.05 (Hughes, 1976)

F = 1.05 x 1408.4 x 3.248
F = 4803 N = 4.803kN

For this design, the Wind load is taken as 4.81 kN.

3.4 Derivation of the Finite Element Method

Using the afore-mentioned preliminary results as necessary pre-requisite data for the complete analysis of the support for the solar collectors; a model of triangular element stiffness matrix for a co-planner (two dimensional) stress formulation was assumed. This method is very popular and well documented by Rao (1989) and Nwofor (2012) and many others authors. Therefore, some essential features of this process are presented in this paper as represented in Figure 2 for the local and global coordinates and nodes numbering for a co-planner elastic triangular element.

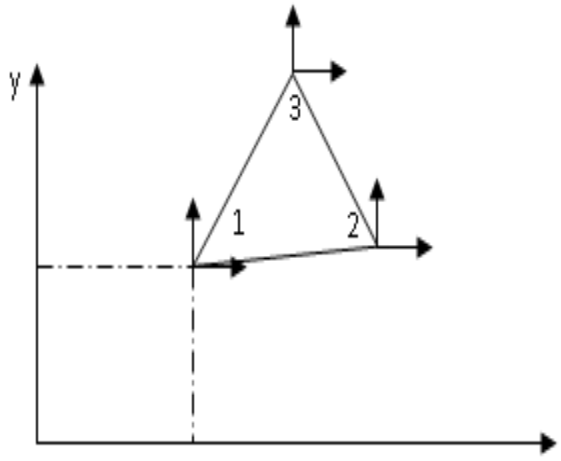

Figure 2: Local and Global Coordinates and Nodes of Nodal Forces and Displacements

Typical co-planner nodes have two components of displacements $\delta_i = \begin{Bmatrix} u_i \\ v_i \end{Bmatrix}$ and this consequently produces corresponding force vectors $\{F_i\} = \begin{Bmatrix} f_{xi} \\ f_{yi} \end{Bmatrix}$. Therefore, the complete force and displacement vectors are represented by equation (9).

$$\{\delta^e\} = \begin{Bmatrix} u_1 \\ v_1 \\ u_2 \\ v_2 \\ u_3 \\ v_3 \end{Bmatrix} \quad (9)$$

$$\{F^e\} = \begin{Bmatrix} F_{x1} \\ F_{y1} \\ F_{x2} \\ F_{y2} \\ F_{x3} \\ F_{y3} \end{Bmatrix} \quad (10)$$

For this triangular element, the stiffness matrix $[K^e]$ produces a square matrix of 6x6 from equation (11) (Nwofor, 2012):

$$\{F^e\} = [K^e]\{\delta^e\} \quad (11)$$

According to Rao (1989), the derivation of element characteristic matrices and vectors involves the integration of the shape functions or their derivatives or both over the element. These integrals can be evaluated easily if the interpolation functions are written in terms of local coordinates systems. The interpolation functions are written in terms of local coordinate system by using the coordinate transformation relation. To achieve this, a suitable displacement function is chosen to define the displacement at any point in the element. This is simply represented by two linear polynomials functions containing six unknown coefficients $(\alpha_1, \alpha_2, \ldots \alpha_6)$ representing the six degrees of freedom in the case of a co-plane triangular element (Nwofor, 2012).

$$u = (\alpha_1 + \alpha_2 x + \alpha_3 y)$$
$$v = (\alpha_4 + \alpha_5 x + \alpha_6 y) \quad (12)$$

The corresponding elasticity material matrix [D] which takes into consideration corresponding contributions of the material Modulus of Elasticity, E and the Poisson ratio, ν to stress and strain is expressed as (Rao 1989 and Nwofor, 2012)

$$[D] = \begin{bmatrix} d_{11} & d_{12} & 0 \\ d_{21} & d_{22} & 0 \\ 0 & 0 & d_{33} \end{bmatrix}$$

IJST © 2013– IJST Publications UK. All rights reserved.

For co-planner stress $\sigma(x,y)$

$$d_{11} = d_{22} = \frac{E}{(1-\nu^2)}$$
$$d_{12} = d_{21} = \frac{\nu E}{(1-\nu^2)}$$
$$d_{22} = d_{33} = \frac{E}{2(1-\nu)} \quad (13)$$

The stresses, $\sigma(x,y)$ and the strain $\varepsilon(x,y)$ at any point on the element are related as (Nwofor, 2012).

$$\{\sigma(x,y)\} = \begin{Bmatrix}\sigma_x\\ \sigma_y\\ \tau_{xy}\end{Bmatrix} = \frac{E}{(1-\nu^2)}\begin{bmatrix}1 & \nu & 0\\ \nu & 1 & 0\\ 0 & 0 & \frac{1-\nu}{2}\end{bmatrix} \quad (14)$$

and the relationship between element stresses and nodal displacement is presented as

$\{\sigma(x,y)\} = [D]\{\varepsilon(x,y)\}$; hence $[D] = [E]$
$\{\varepsilon(x,y)\} = [B]\{\delta^e\}$ and finally
$\{\sigma(x,y)\} = [D][B]\{\delta^e\}$ (15)

Since $[D], [B]$ and $\{\delta^e\}$ are not functions of x and y the elements will have a constant stress distribution along the members directrix. Therefore, the relationship between statically equivalent nodal forces, $\{F^e\}$ nodal displacements, $\{\delta^e\}$ and stiffness matrix, $\{K^e\}$ is $\{F^e\} = \lfloor\int [B]^T [D][B]d(vol)\rfloor\{\delta^e\}$ and triangular stiffness matrix is $\{K^e\} = \lfloor[B]^T[D][B]\Delta t\rfloor$.

For a given strut or tie co-planner element; at the beginning (i) and end (j) , there are two degrees of freedom each, hence, the stiffness matrix corresponding to the axial displacements is given as

$$\{K^e_{4x4}\} = \iiint_{vol}(e)[B]^T [D][B]d(vol).$$

Therefore a given element i j (i.e. bar i j) with dimension, l

$$[B] = \left[-\frac{1}{l} \quad \frac{1}{l}\right] \text{ and } [B]^T = \begin{bmatrix}-\frac{1}{l}\\ \frac{1}{l}\end{bmatrix} \quad (16)$$

and

$$\{K^e_{4x4}\} = \frac{A^e E^e}{l^e}\begin{bmatrix} l_{ij}^2 & l_{ij}m_{ij} & -l_{ij}^2 & -l_{ij}m_{ij}\\ l_{ij}m_{ij} & m_{ij}^2 & -l_{ij}m_{ij} & -m_{ij}^2\\ -l_{ij}^2 & -l_{ij}m_{ij} & l_{ij}^2 & l_{ij}m_{ij}\\ -l_{ij}m_{ij} & -m_{ij}^2 & l_{ij}m_{ij} & m_{ij}^2\end{bmatrix}\begin{matrix}Q_{1\,i-1}\\ Q_{1\,i}\\ Q_{1\,j-1}\\ Q_{1\,j}\end{matrix}$$

$$Q_{1\,i-1} \quad Q_{1\,i} \quad Q_{1\,j-1} \quad Q_{1\,j} \quad (17)$$

Where A^e is the area of the cross section of the element, l_{ij} member length, m_{ij} the corresponding direction cosine of centre line ij and $Q_{1\,i-1}$, $Q_{1\,i}$, $Q_{1\,j-1}$ and $Q_{1\,j}$ are the vectors of nodal displacements of any particular element e in the global coordinate system.

4. PRESENTATION OF RESULTS AND DISCUSSION

The total wind load, F acting on the structure is distributed between the two supports ends and for the purpose of analysis it is assumed to be a point load acting on the members supporting the solar collectors at point B and E of the shaft. Hence, the wind induced loading is 2.41kN for each support and the load from the chain drive is 0.2 kN. Similarly, the loads acting on the support bearings were approximated as 0.86kN and 0.63kN for points B and E respectively.

According to Douglas *et al.* (1980), fluid flow past a body produces Reynolds number (Re) that is proportional to the velocity of the fluid; hence, the Reynolds number varies with variation of velocity. Therefore, at low Reynolds number (e.g. 0.5), the inertia effects are negligible, between 2 and 30, separation of boundary layer occurs with symmetrical eddies rotating in opposition to one another are formed. As the Reynolds number further increases it tends to elongate fixed eddies which then begin to oscillate until about 90; depending on the free stream turbulence level, they break away from the body. As the Re increases, this process is intensified and the formation of wake of discreet rows of vortices is developed. This is known as Vortex Street or Von Karman Vortex Street. At this stage, the contribution of drag profile is three-quarters. The shedding of each vortex produces circulation and hence, gives rise to a lateral force on the body. Since these forces are periodic in nature, the frequency of the vortex shedding lead to the development of forced vibration on the body. This familiar 'singing' phenomenon caused by a lateral wind is the usual cause of the collapse of many structures as a result of resonance between the natural frequency of the body and the frequency of the forced vibration due to vortex shedding. The frequency of such forced vibration, sometimes called self-induced vibration, may be calculated from Vincent Strouhal empirical formula (Douglas *et al.*, 1980).

$$\frac{fB}{V_w} = 0.198\left(1 - \frac{19.7}{R_e}\right) \quad (18)$$

Equation (18) is known as Strouhal number or reduced frequency and the corresponding Reynolds numbers is derived by defining $f = \frac{38.462}{H}$ (Onundi *et al.*, 2011).

IJST © 2013– IJST Publications UK. All rights reserved.

Therefore,

$$R_e = 19.7\left(1 - \frac{0.00515V_wH}{B}\right) \quad (19)$$

Where, H = 1.8m is the model height in meters.

This corresponding Strouhal number is very important for the determination of the frequencies *f*, at which peaks occur, depending on the reduced frequency observed. V_w is the mean basic wind speed and B = D is the width or diameter of the structure (dish) (Kijewski and Kareem 2001 and Kareem 1982).

The turbulent boundary layers simulated in this study were generated by the natural action of surface roughness added on the tunnel floor and by upstream spires when tested in a wind tunnel. Two approach flows, namely, BL1 (α =0.16) and BL2 (α = 0.35), where α = exponent of mean wind velocity profile, corresponding respectively to an open and urban wind environments (Kijewski and Kareem, 2001). Unlike the along spectrum, the across-wind spectrum exhibits an evident peak around the Strouhal number (i.e. when Reynolds (Re) is within 250< Re < $2x10^5$, Douglas (1983)) which for this model corresponds to Reynolds number of 13.2 for the defined peak of reduced frequency of 1.08.

In this case, the possibility of negative aerodynamic damping, a manifestation of motion-induced effects, may not cause the computed results to be inaccurate due to the influence of the prevailing wind speed. Therefore, the work on wind load spectra will be limited to the high reduced frequency range since $f^* = \frac{fD}{V_w} = 1.08 > 0.1$ which encompasses the wind velocity of operation of most tall buildings and other flexible structures. The amplitude and bandwidth of the spectrum depend mainly on the side ratio, although generally, the higher the peak value, the narrower the spectrum. The torsional and across wind Root Mean Square (RMS) moment coefficient is very sensitive and markedly depends on the side ratio, but increased turbulence yields markedly large base moment coefficients side ratio D/W < 1.0, while the sensitivity to aspect ratio is only moderate and substantially diminished for 1.5 ≤ D/W ≤ 2.0 (Kijewski and Kareem, 2001) which corresponds to the existing study. Flexible structures that may be sensitive to dynamic effects and wind–excitation oscillations such as vortex shedding; structures typical are those with a height - to- width ratio greater than 5, and over 122m in height (but the BS6399, 2004 allows for up to but not more than 300m and augmentation factors, C_r less than 0.25) or frequency of vortex shedding in Hertz, f.

In selecting the dimensions of the structural support members that satisfy the stresses, deflections and other serviceability requirements, the solutions were digitized for analysis using RISA 3D (Rapid Interactive Structural Analysis for 3 Dimensional Systems) Software which is based on the application of the finite element method. The schematic diagram of the digitized and visualized structural support that was found satisfactory is shown in Figure 3. Details of input; local and global coordinates, member data, Boundary Conditions, basic load case data, member point load, joint displacement, joint loads, and load combinations were carried out and the results are summarised as follows:

A single 25 x 25 x 3mm (1.2kg/m) equal angle iron proved adequate and satisfactory for all the members except the shaft which is CHS48.3x5(48.3mm, external diameter; 5mm wall thickness; 680mm^2, area of the section and 162000 mm^4,moment of inertia) shown in Figures (3 and 4). The equal angle iron has a total length of 22.3m weighing 27.5 kg and the shaft 1.5m weighing 8kg. The rectangular grids and the triangular braces and wind lattices were carefully arranged to ensure triangular formations to ensure that the supports systems are stable and geometrically instantaneously unmovable.

Support structure for solar bi-focal collectors system was achieved by coupling the different elements of the structure such as the longitudinal and transverse members as rectangular grids of the base and stem of the supports. Wind –lattices inform of lateral ties and diagonal struts were coupled with the receivers and support arms to the rotating support all fastened together using conventional mechanical friction bolts and nuts to allow for an onsite easy assembling and dismantling. Also tested were corresponding frequencies to the first, second and third modes of vibration which are 25.3, 41.4 and 57.1Hz meaning periods of 0.04, 0.024 and 0.18 seconds respectively. A maximum of 1.51mm horizontal displacement was computed for the whole system and this was registered at node number N6 and a maximum stress of 39.4 MPa (i.e. 39.4 Nmm^{-2}) occurred along member M12 due to the influence of bending moment. These computed low levels of displacements, stresses and frequencies, periods, Reynolds and Strouhal numbers show that neither excessive stresses nor deformation or vibrations may disturb the excellent and efficient performance of the bi-focal solar collectors.

IJST © 2013– IJST Publications UK. All rights reserved.

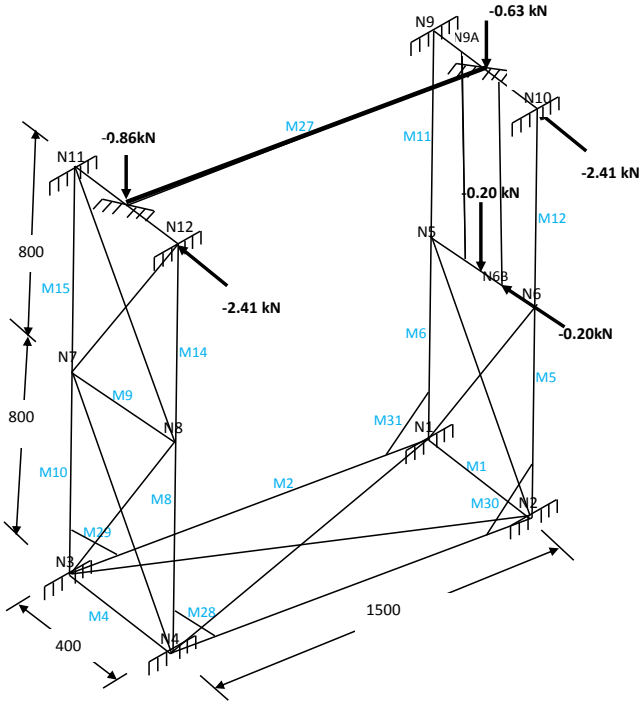

Figure 3: Geometry of the Structural Support

Figure 4: Support Structure of Solar Tracking Bi-Focal Collector System on Field Test.

IJST © 2013– IJST Publications UK. All rights reserved.

5. CONCLUSION AND RECOMMENDATIONS

In this study, support structure for solar tracking bi-focal collectors which comprise of rotating shaft, mild steel support structure for two number solar collectors and support frame structure which permits azimuth rotation of the support shaft and collective rotation of the solar collectors was designed. The support structure of solar tracking bi-focal collector system was satisfactorily concepted, designed and analysed. All the component parts were carefully assessed and detailed analysis were carried out by considering a wide range of extreme loadings of both static and dynamic excitations to ensure they complied with the deemed to satisfy requirements of the serviceability limit state of such structural systems.

Procedure recommended by the American Institute of Steel Construction (AISC) was followed in the design of the support structure while RISA 3D software was introduced for the analysis of the structural members in relation to the load components. A single 25 x 25 x 3mm (1.2kg/m) equal angle iron proved adequate and satisfactory for all the members except the shaft which is CHS48.3x5mm (5.34kg/m). No excessive stress, deformation or any other related dynamic sensitive considerations proved to have adverse influence on the structural stability, durability, reliability or quality assurance capabilities of the solar tracking system. Therefore, the under laid studies and procedures, are recommended for the design of similar solar tracking bi-focal collector support systems with larger magnitudes anywhere in the World; so far, the local conditions are considered for locality sensitive parameters (e.g. basic wind speed etc.) for such structural analysis and design. It must also be recognized that design Codes of practice and the magnitude of yield stress and Young modulus of elasticity of materials may vary from country to country; these facts, must be complied with and necessary modifications discretely incorporated while using the softwares for solving such engineering problems.

REFERENCES

[1] **Abdulrahim, A.T., Diso, I.S. and Olalere, R.K. (2012),** "Development of an Automated Tracking Device with Bi-Focal Solar Collector". Journal of Engineering Research, 17(3), 1-11.

[2] **Ajiya M. (1995).**"Design and Construction of a Parabolic Solar Cooker". Unpublished B.Eng. Project, Mechanical Engineering Department, University of Maiduguri.

[3] **Allen S. H., Alfred, R. H. and Herman G. L. (1982).** "Theory and Problems of Machine Design". McGraw Hill Book Company, Singapore.

[4] **Asante–Nimako M. (1988).**"Wind Load Estimation for Structures in Nigeria". Technical Paper, Structural Engineering, Vol. 1, pp. 16 – 21.

[5] **British Standard Institution, Loadings for Buildings (1977).** "Code of Practice for Wind Loads", CP3 Chapter V, Part2, Building and Civil Engineering Sector Board, United Kingdom.

[6] **British Standard, Loadings for Buildings (B.S. 6399)- Part 2. (2005).** "Code of Practice for Wind Loads (as Amended)", Building and Civil Engineering Sector Board, United Kingdom.

[7] **Cooper P. T. (1972).** "Solar Energy". Macmillan Press Limited, England.

[8] **Dahiru D. Y., Malachy S. and Asese A. A. (2007)**. "The Development of a Concentrating Solar Energy Cooker under Hazy Weather Condition". Journal of Scientific and Industrial Studies, 5 (2): 25 - 32.

[9] **Duffie J. A. and Beckman J. M. (1974).** "Solar Energy Thermal Processes". A Wiley Inter-science Publication, London.

[10] **Douglas, J.F., Gasiorek, J.M. and Swaffield, J.A. (1980)**. "Fluid Mechanics", A Pitman International Text. Longman Group Ltd. U.K.

[11] **Hughes B. P. (1976).** Limit State Theory for Reinforced Concrete Design. The Pitman Publishing Limited, 2nd Edition, London.

[12] **Kareem, A. (1982).** "Lateral – Torsional Motion of Tall Buildings to Wind Loads". J. Struct. Engrg., ASCE, 111 (11), 2479-2496.

[13] **Khurmi R. S. and Gupta J. K. (2004).** "A Text book of Mechine Design". Eurasia Publishing House (Put.) Ltd., Ram Nagar, New Delhi – 110005.

[14] **Kijewski, T and Kareem, A (2001).** "Dynamic Wind Effects: A Comparative Study of Provision in Codes and Standards with Wind Tunnel Data", Tracy.L.Kijewski.1@nd.edu , Notre Dame

[15] **Nwofor, T.C. (2012).** "Numerical Modeling of Brick-Mortar Couplet", Continental Journal of Environmental Design and Management 2 (1): 1 - 9, 2012 ISSN: 2251 – 0478. Retrieved on 28th October, 2012 from http://www.wiloludjournal.com, doi:10.5707/cjedmgt.2012.2.1.1.9

[16] **Magal B. S. (1993).** "Solar Power Engineering". Tata Mc Graw – Hill publishing company limited, New Delhi, India.

IJST © 2013– IJST Publications UK. All rights reserved.

[17] **Mshelbwala S. A. (1996).** "Experimental Evaluation of a Parabolic Solar Cooking Device". Unpublished B.Eng. Project, Mechanical Engineering Department, University of Maiduguri.

[18] **Muller- Steinhagen H. (2003).** "Concentrating Solar Power: A Vision for Sustainable Electricity Generation". www.ecm.auckland.ac.nz/conf/Auckland-2.pdf

[19] **Onundi, L. O. (2010).** "The Impact of Climate Change on Sustainable Infrastructural Development - A Case Study of the Appropriate Wind Speed and other Measures Required for Design of Tall Structures In Nigeria". A Paper Presented to the Council for Regulation of Engineering in Nigeria 2010 Assembly (2010 COREN Assembly). Abuja.

[20] **Pelemo D. A., Fasasi M. K., Owolabi S. A. and Shaniyi J. A. (2002 a).** "Design, Construction and Performance of Focusing Type Solar Cooker". Nigeria J. of Physics Vol. 4, No.2, pp. 109 – 112.

[21] **Rao, S.** S. **(1989).** "The Finite Element Method in Engineering", Published by Pergamon Press, Second Edition. Oxford.

[22] **Shigley J. E. and Mischke C. R. (2001).** "Mechanical Engineering Design". McGraw Hill Companies, Inc. 6th Edition, New York.

[23] **Soboyejo, A.B.O. (1971).** "Distribution of Extreme Winds in Nigeria", The Nigerian Engineer, Vol. 7, No, 3, pp. 21 – 34.

IJST © 2013– IJST Publications UK. All rights reserved.